Figures

NOTE: This information is distributed solely for the purpose of pre-dissemination peer review under applicable information quality guidelines. It has not been formally disseminated by the U.S. Environmental Protection Agency. It does not represent and should not be construed to represent any agency determination or policy.

Figures for Chapter 6, Wild and Scenic Rivers

Figure 6.1. Photo of Snake River below Hell's Canyon Dam. Photograph compliments of Marshall McComb, Fox Creek Land Trust.

Figure 6.2. Wild and Scenic Rivers in the United States. Data from USGS, National Atlas of the United States (2005).

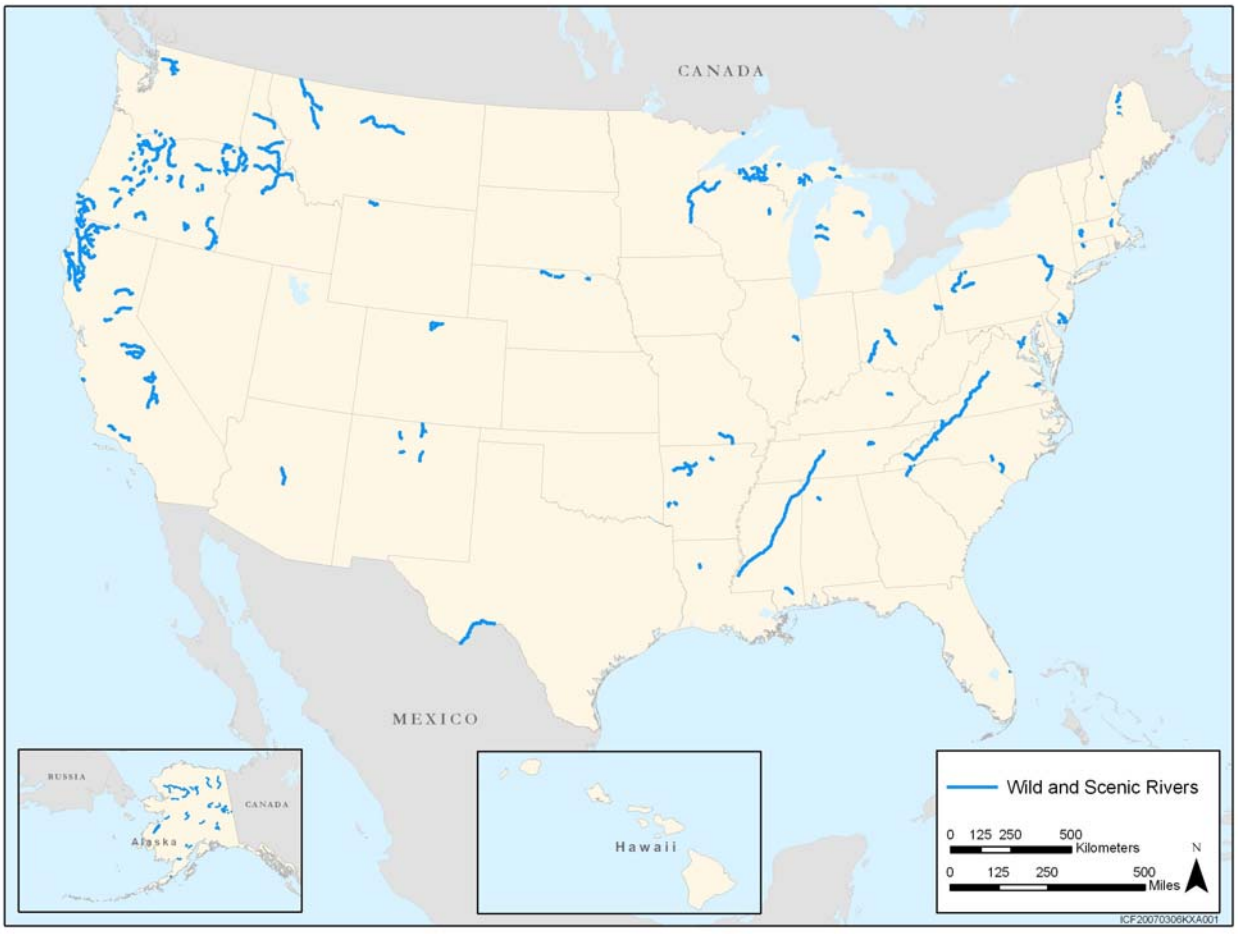

Figure 6.3. Selected milestones in the evolution of the Wild and Scenic Rivers system. Adapted from National Wild and Scenic Rivers System website (2007a).

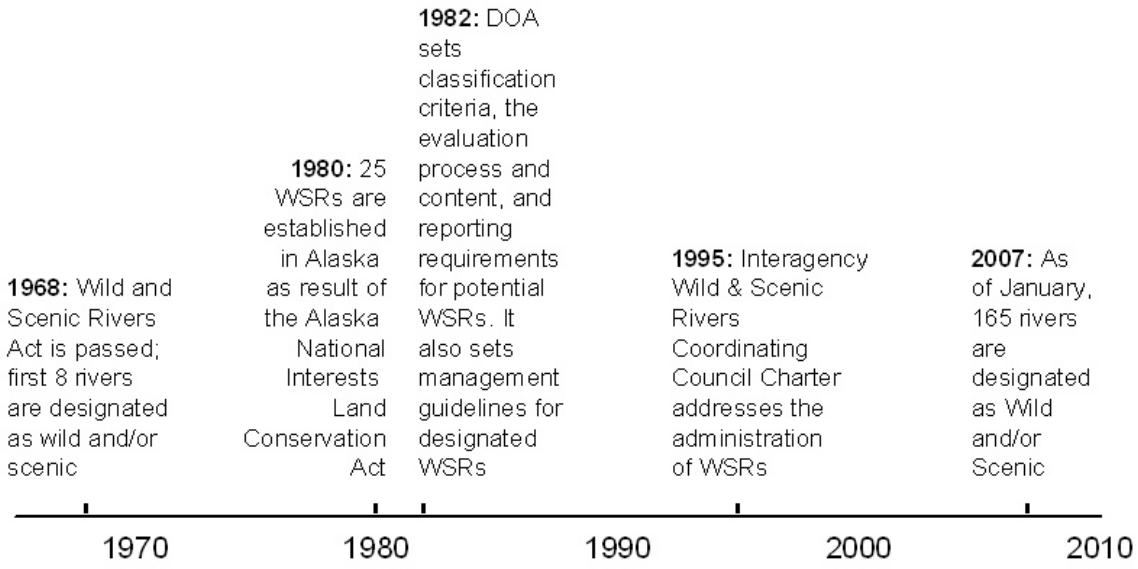

Figure 6.4. Conditions and factors affecting the future conditions of Wild and Scenic Rivers.

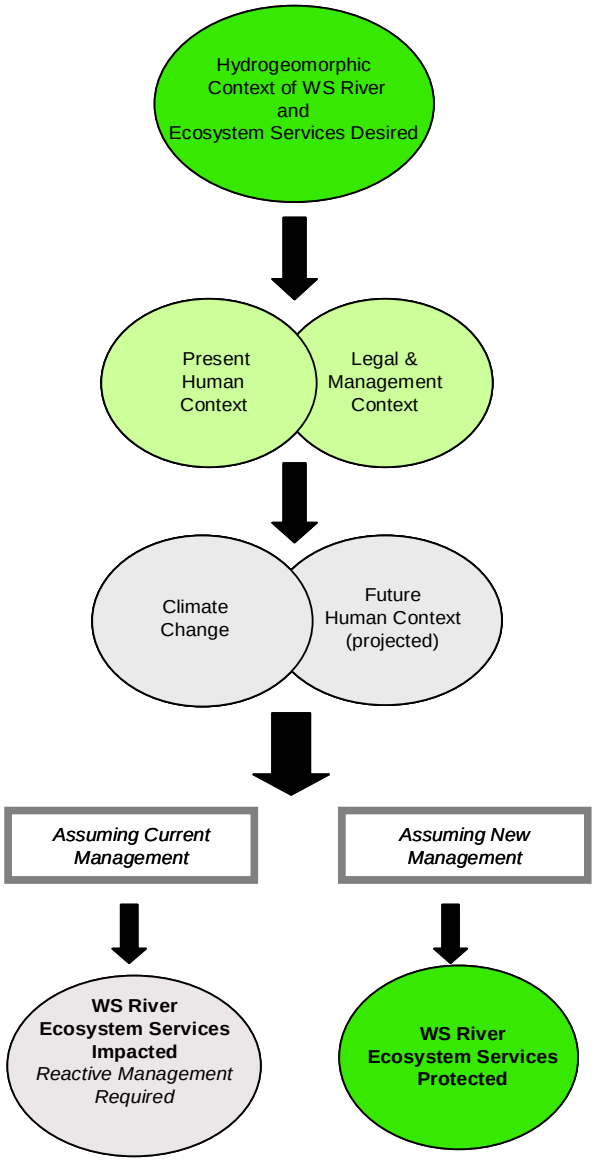

Figure 6.5. Illustration of natural flow regimes from four unregulated streams in the United States, (a) the upper Colorado River (CO), (b) Satilla Creek (GA), (c) Augusta Creek (MI), and (d) Sycamore Creek (AZ). For each the year of record is given on the x-axis, the day of the water year (October 1 – September 30) on the y-axis, and the 24-hour average daily streamflow on the z-axis (Poff and Ward, 1990).

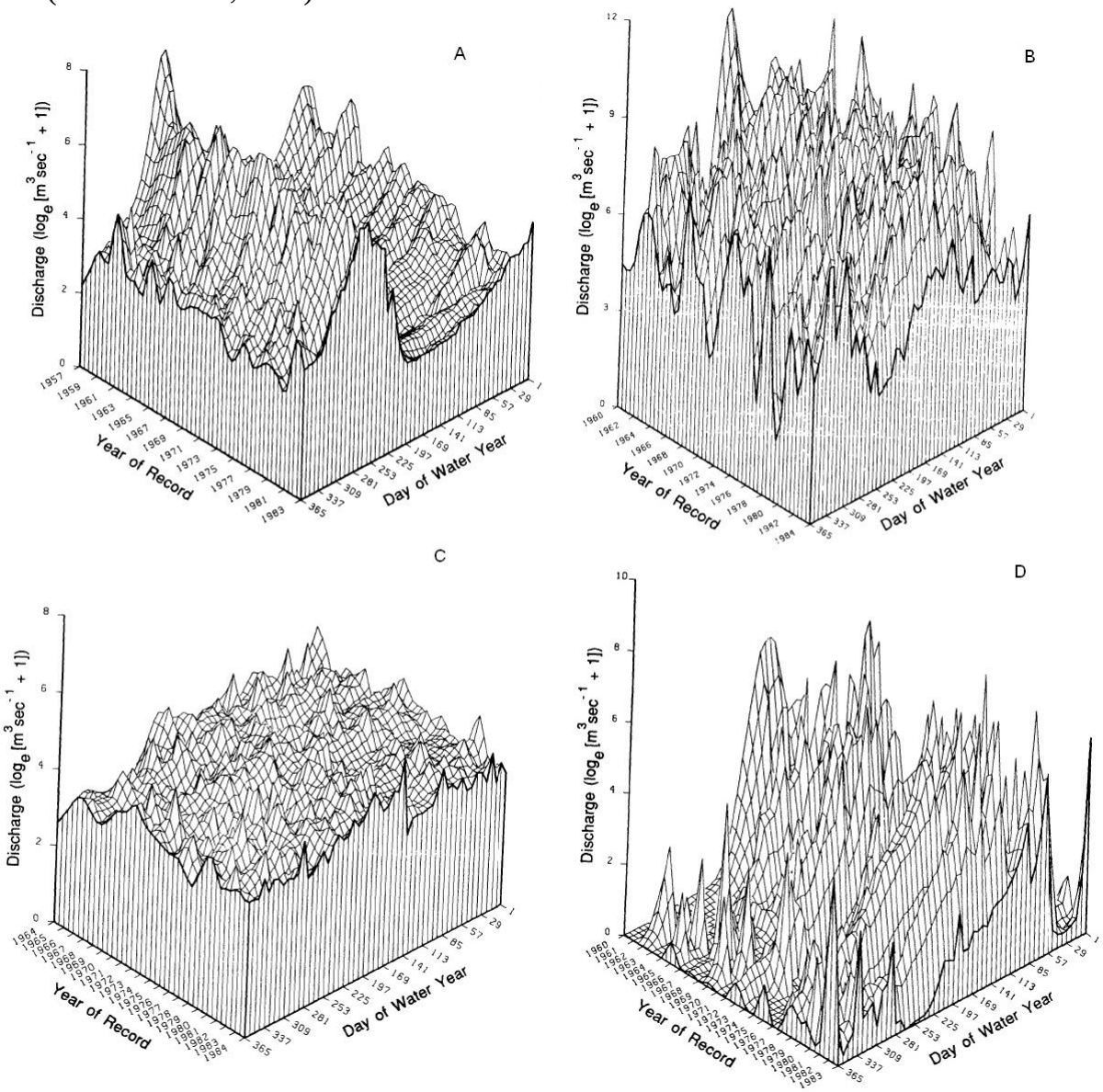

Figure 6.6. Trends in water withdrawals by water-use category. As the population has grown, water has been increasingly withdrawn for public use since 1950 as indicated by total withdrawals (blue line). Water withdrawn for power production and water for irrigation represent largest use followed by water for industrial uses then public supply. From Hutson *et al.* (2004).

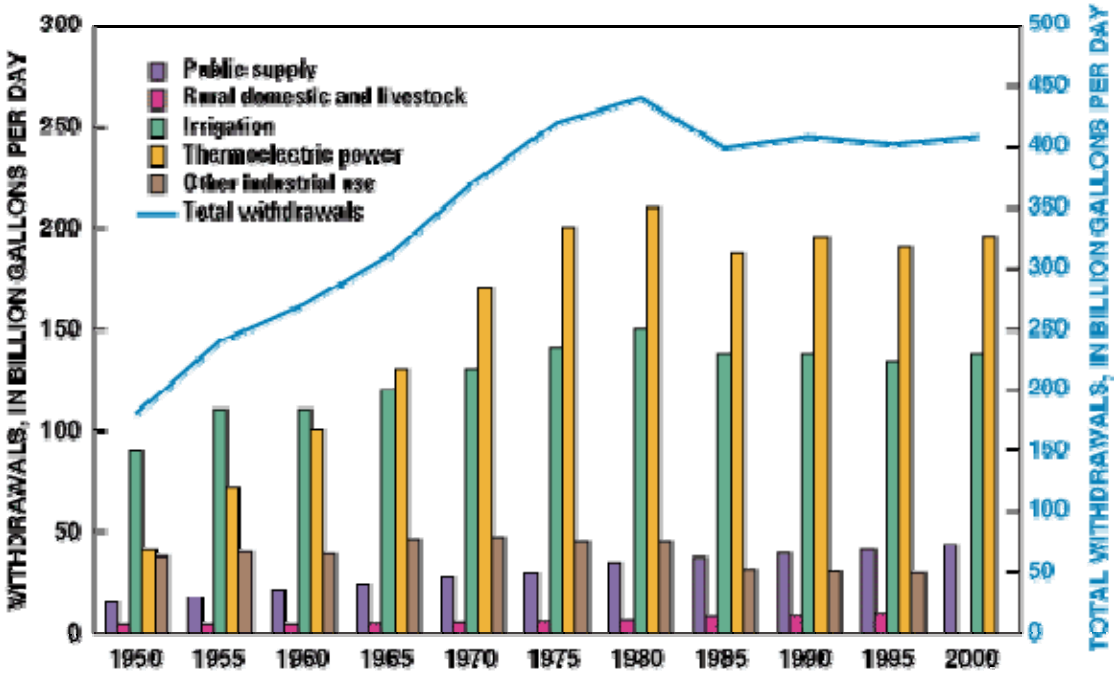

Figure 6.7. Changes in monthly average river flows on the Delaware River, in the Upper Delaware Scenic and Recreational River segment. Lowered flows in December–July result from upstream depletions for New York City water supply. Increased flows result from upstream reservoir releases during summer months for the purpose of controlling salinity levels in the lower Delaware. Figure based on data provided by USGS (2007).

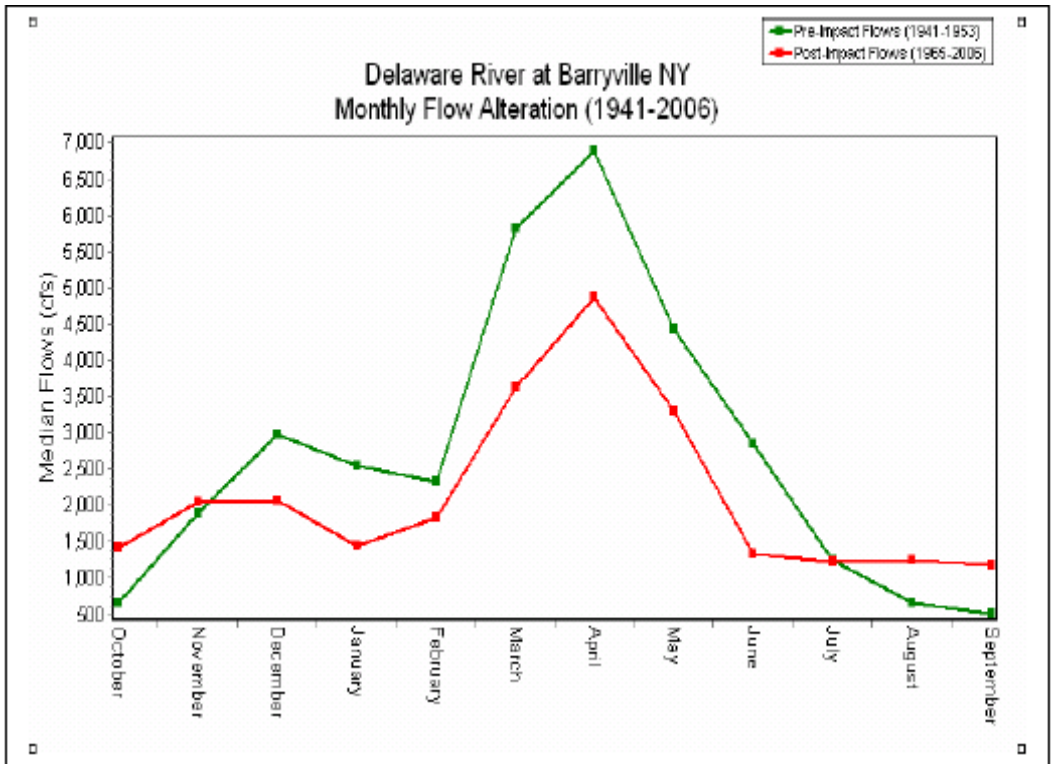

Figure 6.8. Location of dams and WSRs in the United States. Data from USGS, National Atlas of the United States (U.S. Geological Survey, 2005; 2006a).

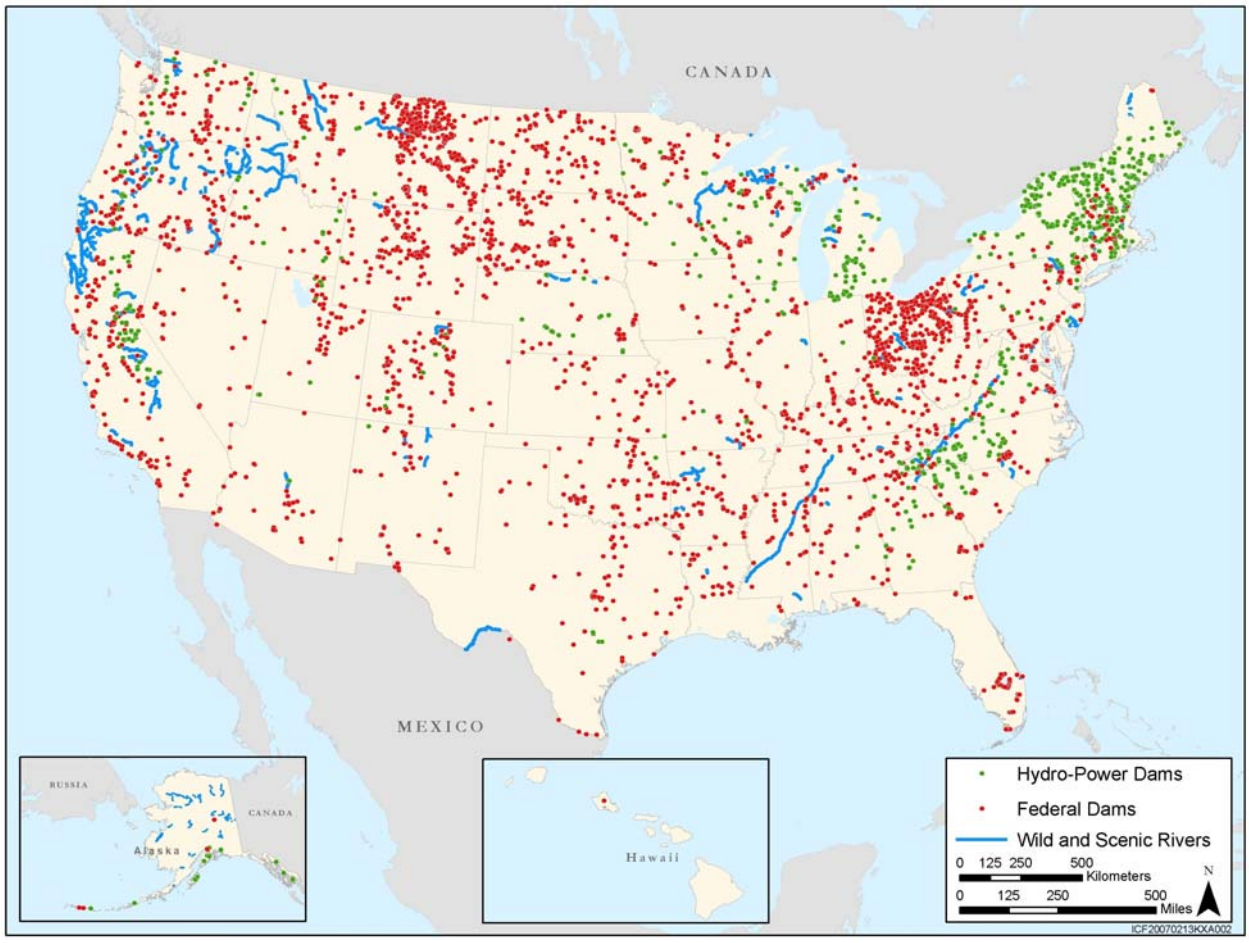

Figure 6.9. Photo of scientists standing on the bed of an urban stream whose channel has been incised more than 5 m due inadequate storm water control. Incision occurred on the time scale of a decade but the bank sediments exposed near the bed are marine deposits laid down during the Miocene epoch. Photograph courtesy of Margaret Palmer.

Figure 6.10. Organization of the WSR system. Adapted from National Wild and Scenic Rivers System website (2007a).

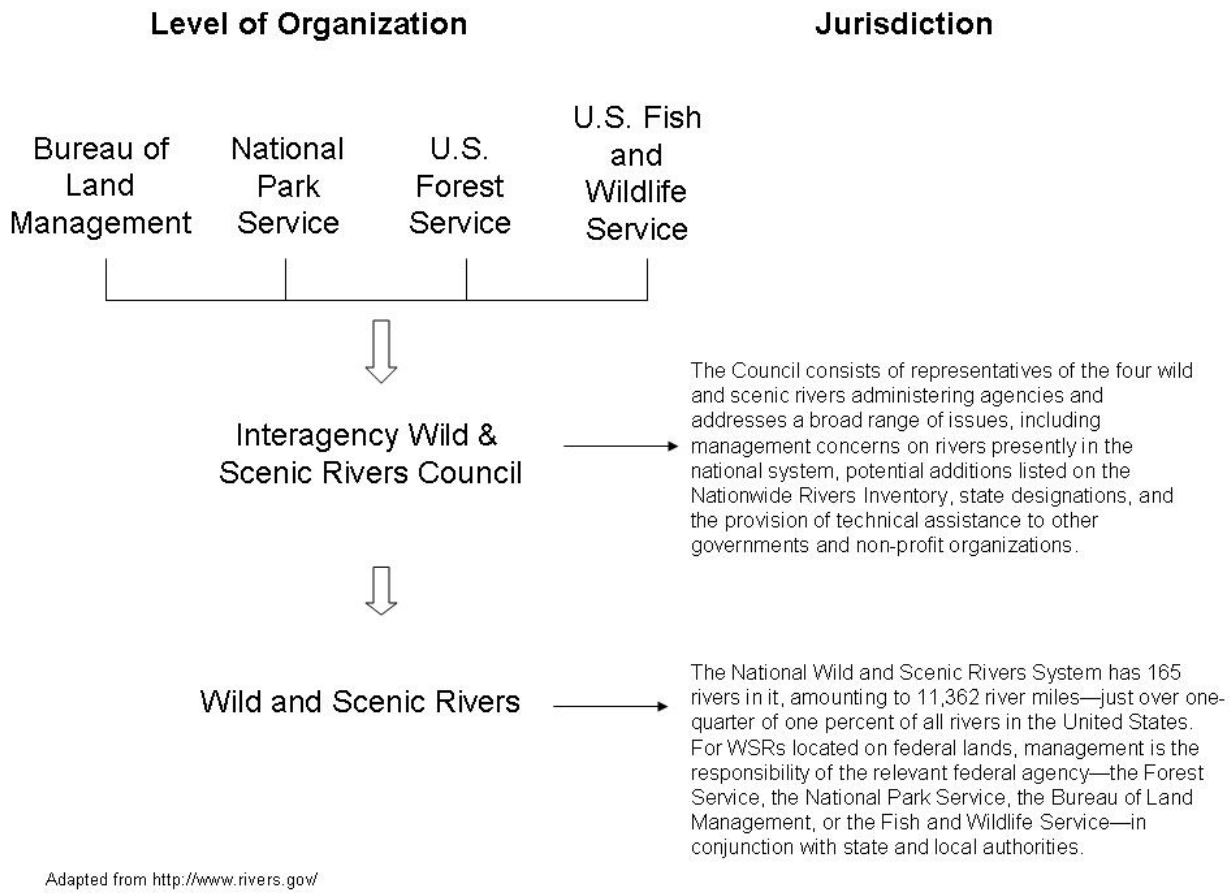

Figure 6.11. Farmington WSR. Photo compliments of the Farmington River Watershed Association.

Figure 6.12. Projected temperature changes for 2091-2100 (University of Arizona, Environmental Studies Laboratory, 2007).*

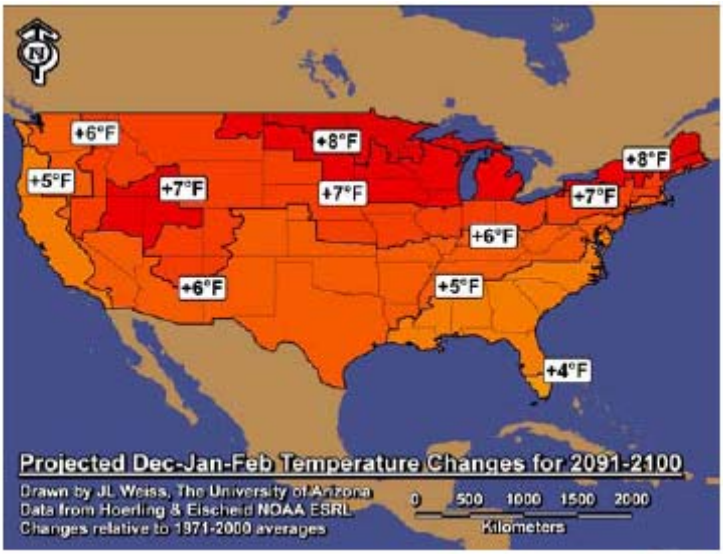

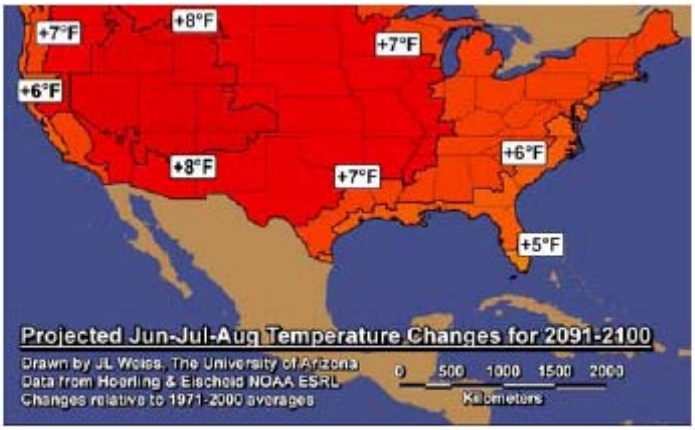

(www.geo.arizona.edu/dgesl/research/regional/projected_US_climate_change.htm

* Note: This figure is provisional, based on securing permission to reprint.

Figure 6.13. Projected annual precipitation changes for 2091-2100 (University of Arizona, Environmental Studies Laboratory, 2007).

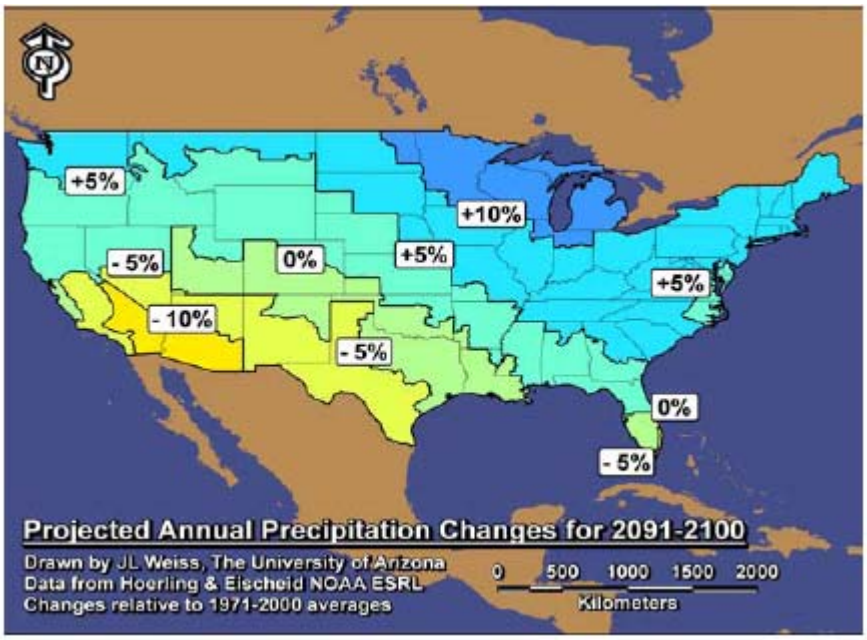

* Note: This figure is provisional, based on securing permission to reprint.

Figure 6.14. Median, over 12 climate models, of the percent changes in runoff from United States water resources regions for 2041–2060 relative to 1901–1970. More than 66% of models agree on the sign of change for areas shown in color; diagonal hatching indicates greater than 90% agreement. Recomputed from data of Milly, Dunne, and Vecchia (2005) by Dr. P.C.D. Milly, USGS.

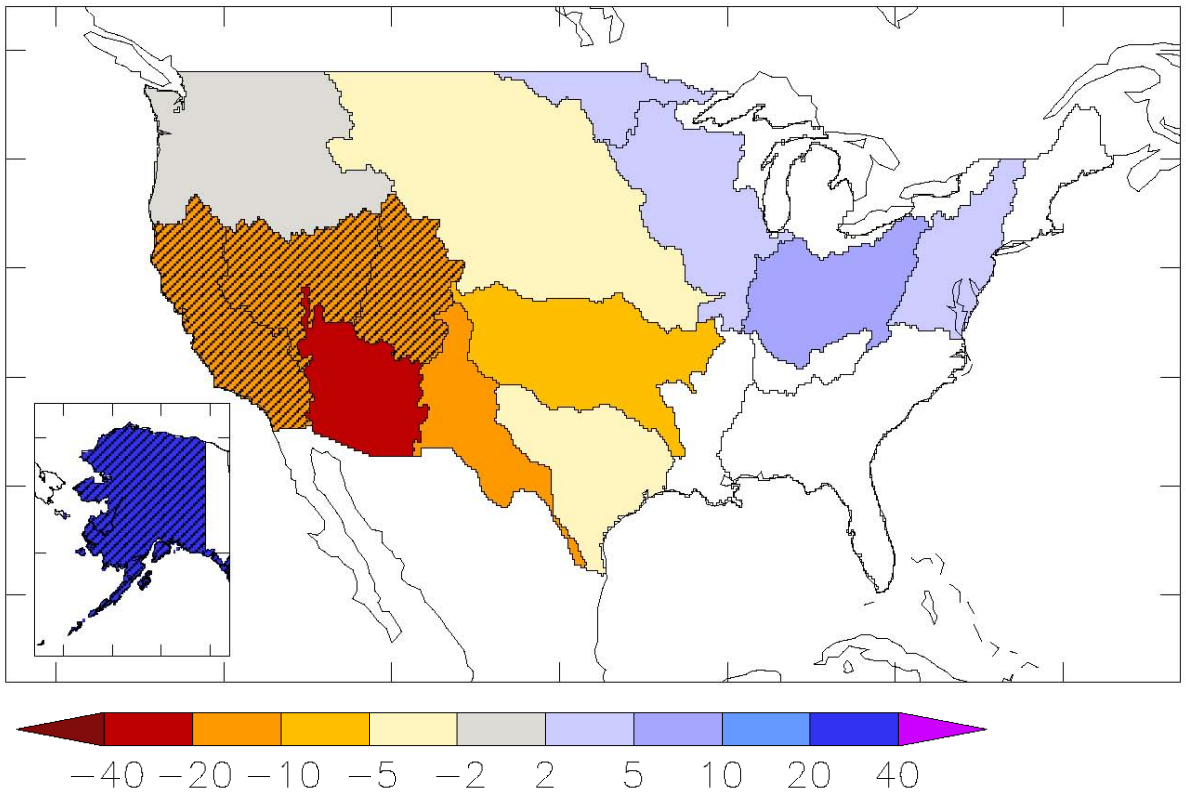

Figure 6.15. Photo of snowmelt in WSR during winter-spring flows. Photo courtesy of National Park Service, Lake Clark National Park & Preserve.

Figure 6.16. Earlier onset of spring snowmelt pulse in river runoff from 1948–2000. Shading indicates magnitude of the trend expressed as the change (days) in timing over the period. Larger symbols indicate statistically significant trends at the 90% confidence level. From Stewart, Cayan, and Dettinger (2005).

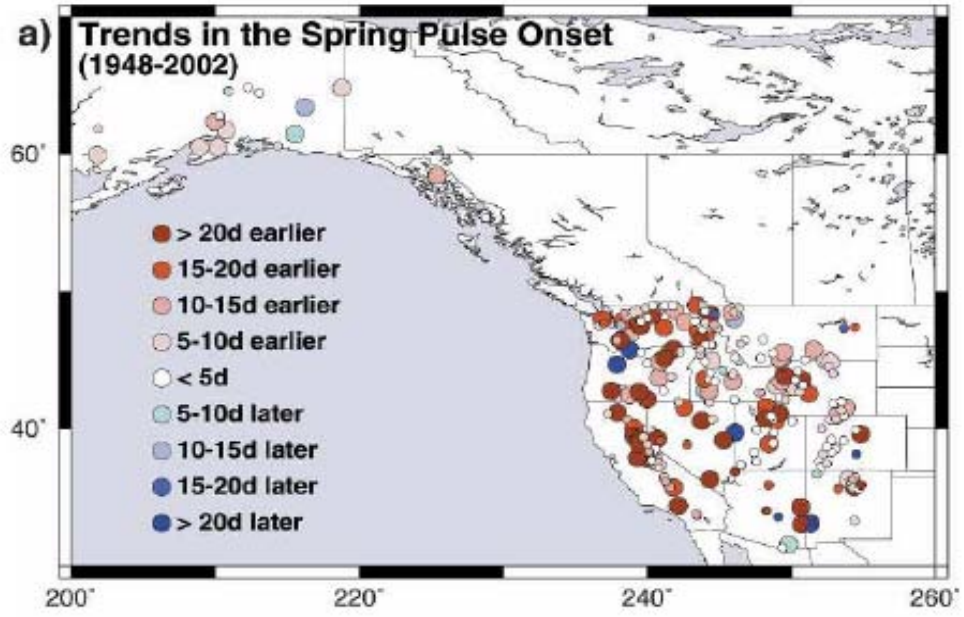

Figure 6.17. Very rapid increases (1–4 hours) in water temperature (temperature "spikes") in urban streams north of Washington D.C. have been found to follow local rain storms. *Top graph:* dark line shows stream discharge that spikes just after a rainfall in watersheds with large amounts of impervious cover; gray line shows temperature surges that increase 2–7ºC above pre-rain levels and above streams in undeveloped watersheds in the region. There is no temperature buffering effect that is typical in wildlands where rain soaks into soil, moves into groundwater, and laterally into streams. *Bottom graph:* shows that the number of temperature surges into a stream increases with the amount of impervious cover. From Nelson and Palmer (2007).

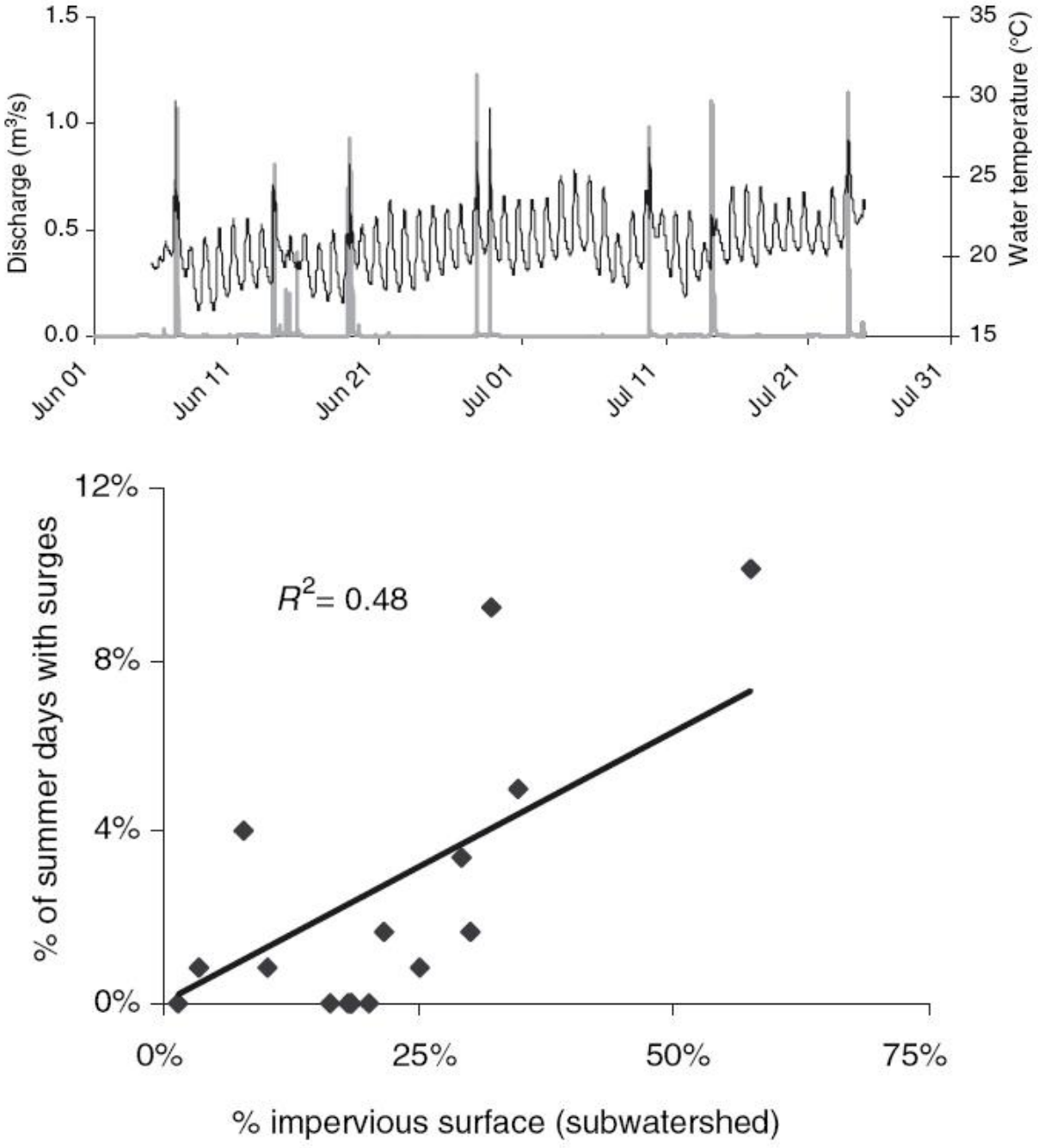

Figure 6.18. Water stress projected for the 2050s based on withdrawals-to-availability ratio, where availability corresponds to annual river discharge (combined surface runoff and groundwater recharge). From Alcamo, Flörke, and Märker (2007).

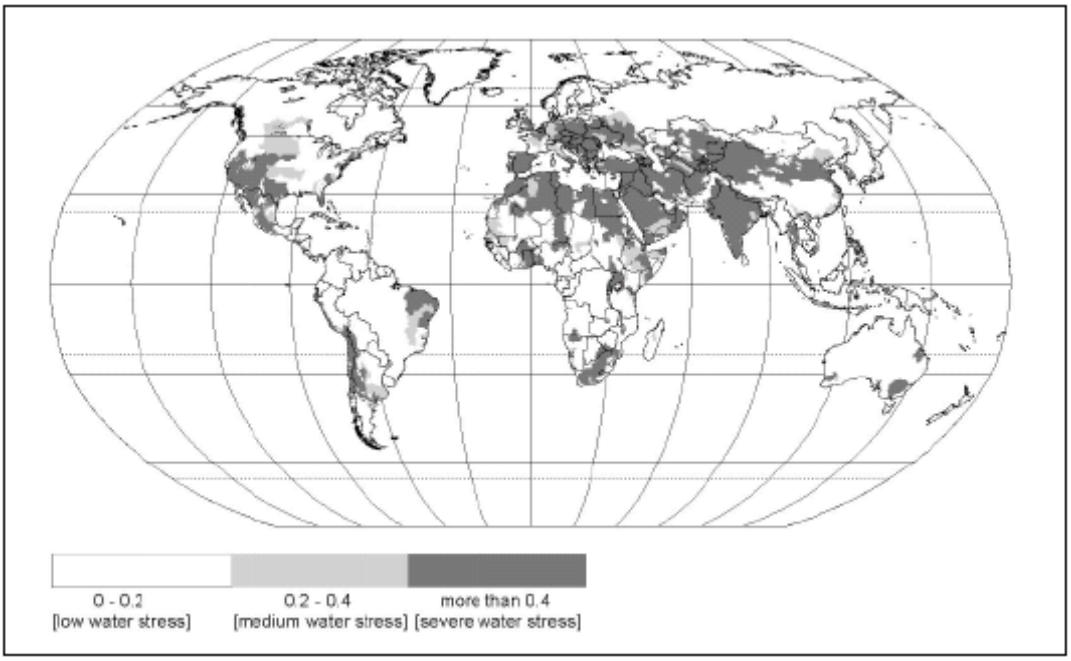

Figure 6.19. The Wild and Scenic portions of the Wekiva River. Data from USGS, National Atlas of the United States (2005).

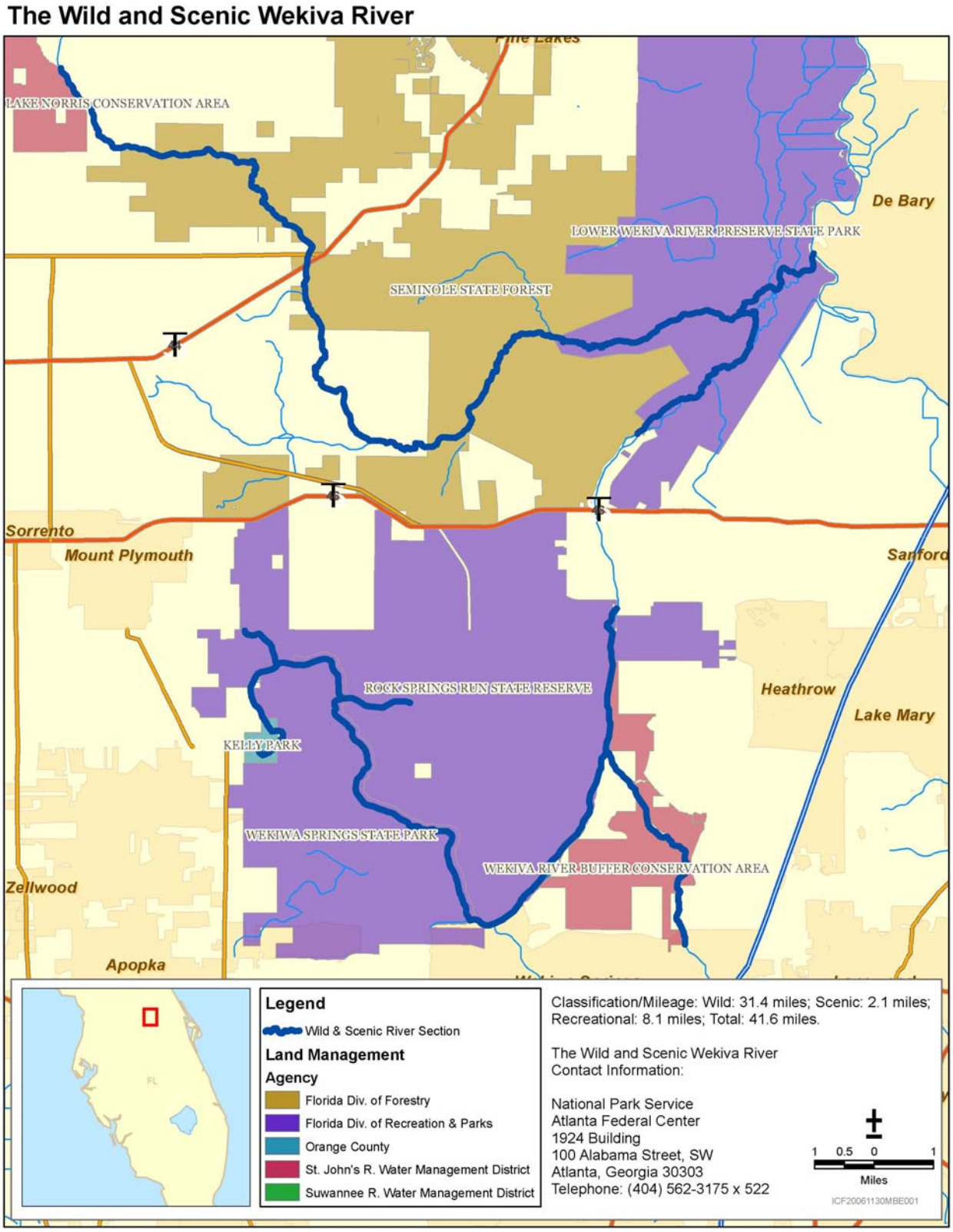

Figure 6.20. The Wild and Scenic portions of the Rio Grande WSR in New Mexico. Data from USGS, National Atlas of the United States (2005).

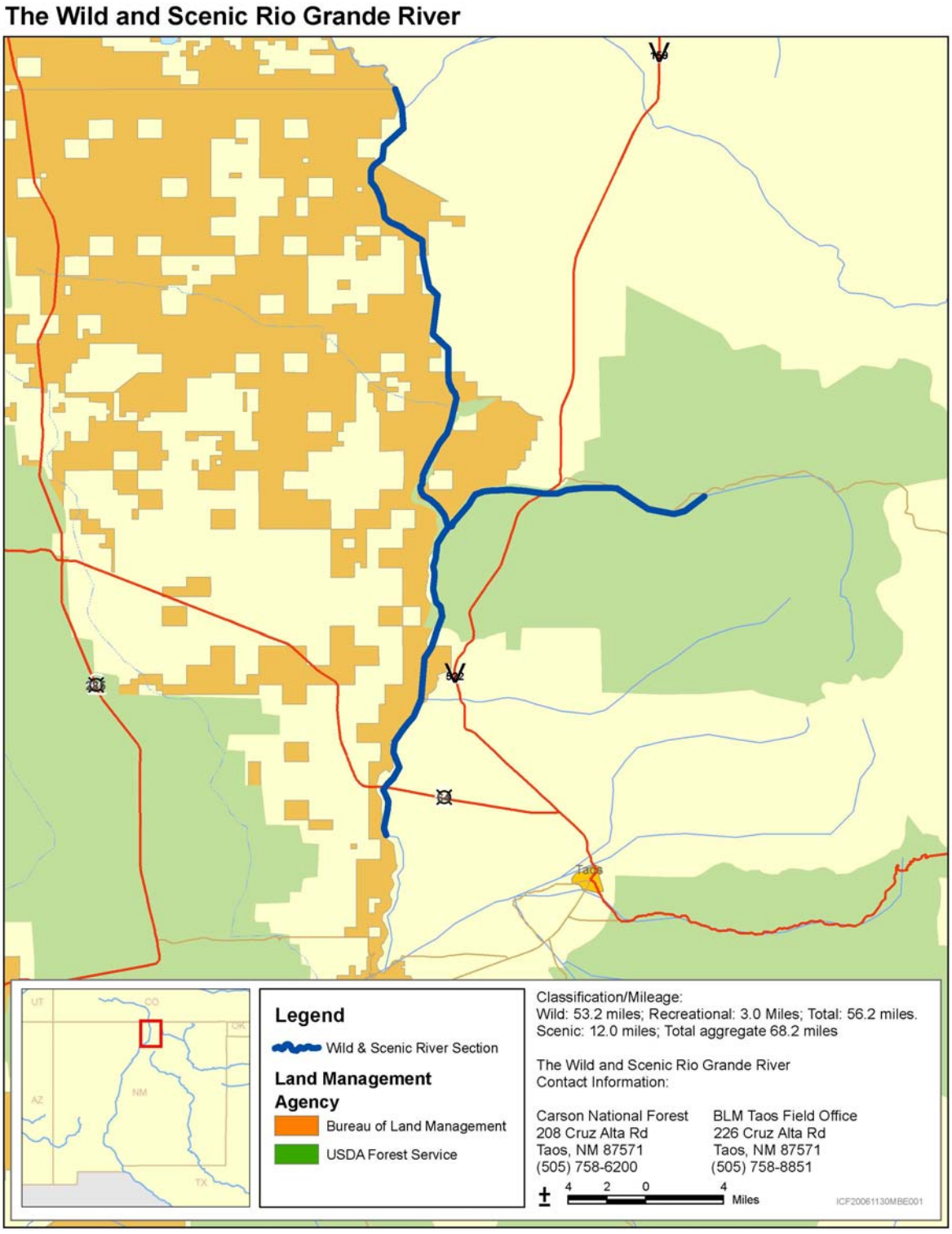

Figure 6.21. The Wild and Scenic portions of the Rio Grande WSR in Texas. Data from USGS, National Atlas of the United States (2005).

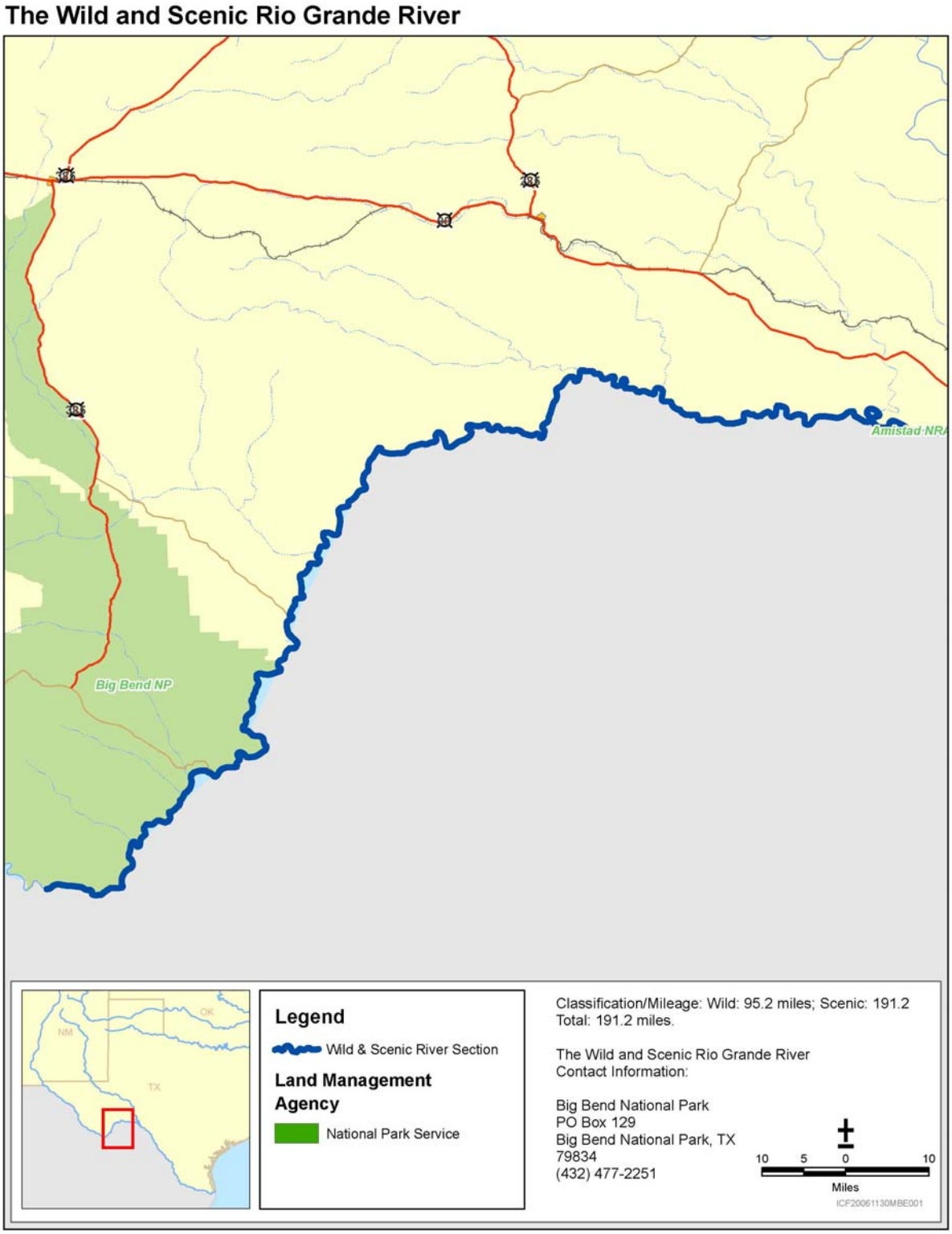

Figure 6.22. Dams and diversions along the Rio Grande (Middle Rio Grande Bosque Initiative, 2007).

Figure 6.23. Map of Wild and Scenic stretches in the Delaware River basin. Courtesy of Delaware River Basin Commission (Delaware River Basin Commission, 2007).